Astron. Astrophys. 315, L285–L288 (1996)

ASTRONOMY
AND
ASTROPHYSICS

Extended fine structure and continuum emission from S140/L1204[1]

R. Emery[1], P. Aannestad[2], N. Minchin[3], S.J. Unger[1], J.-P. Baluteau[4], M.J. Barlow[5], E. Caux[6], G. Serra[6], M. Joubert[7], D. Lorenzetti[8], D. Pequignot[9], C. Armand[10], M. Burgdorf[10], A. di Giorgio[10], C. Gry[10,4], T. Lim[10], S. Molinari[10], D. Texier[10], S.D. Sidher[10], N. Trams[10], B. Swinyard[1], K. King[1], H. Smith[11], I. Furniss[5], D. Ewart[10], M. Price[10], and A. Smith[10]

[1] Space Science Department, Rutherford Appleton Lab, Chilton, Oxon OX11 0QX, UK
[2] Department of Physics and Astronomy, Arizona State University, Tempe, USA
[3] Department of Physics , Queen Mary and Westfield College, Mile End Road, London, E1 4NS, UK
[4] Laboratoire d'Astronomie Spatiale de CNRS, Marseille, France
[5] Department of Physics and Astronomy, University College London, Gower Street, London, UK
[6] Centre d'Etude Spatiale des Rayonnements, 9 Avenue de Colonel Roche, F-31029 Toulouse, France
[7] CNES, 2 place Maurice Quentin, F-75001 Paris, France
[8] Observatorio Astronomico di Roma, Monteporzio, Italy
[9] Section d'Astrophysique, Observatoire de Paris, Paris, France
[10] LWS Instrument Dedicated Team, VILSPA, PO Box 50727, E-28080 Madrid, Spain
[11] National Air and Space Museum, Smithsonian Institute, Lab. Astrophysics, Washington, DC 20560, USA

Received 5 August 1996 / Accepted 13 August 1996

Abstract. Grating spectra, covering the wavelength range 45 to 187μm have been taken with the ISO Long Wavelength Spectrometer (LWS) at a series of pointing positions over the S140 region, centred on the cluster of embedded young stellar objects at the south-west corner of the L1204 molecular cloud. Extended emission from [CII]158μm and [OI]63μm is seen, peaking near the position of the embedded stars. The measurements of the fine structure lines are interpreted in terms of PDR models for the emission, as well as the underlying thermal continuum for the heated gas and dust.

Key words: ISM: S140 – HII regions – ISM: clouds – infrared: interstellar: lines – infrared: interstellar: continuum

1. Introduction

The BOV star, HD211880, at a distance of 910 pc (Crampton and Fisher 1974), illuminates the south-west side of the molecular cloud (L1204) to produce a visible HII region S140, an ionization front (IF), and a photodissociation region (PDR) which appears to be seen edge-on. It is likely that the star represents an earlier phase of star formation activity in the cloud and now a new (sequential) phase of star formation is apparent with young stellar objects (S140 IRS1,2,3) with IRS1 being a bipolar outflow source embedded in the cloud behind the ionisation front (Minchin et al., 1995a and references therein).

Extended mapping of CO ($J = 1 \rightarrow 0$) emission over the region has previously been made by Blair et al. (1978), and of [CI] at 492 GHz and ^{13}CO ($J = 2 \rightarrow 1$) by Plume et al. (1994). The embedded source region has been mapped at high resolution in [CI], C^{17}O, ^{13}CO and C^{18}O emission by Minchin et al. (1994 and 1995b) to include the bipolar outflow and the PDR to the south-west, adjacent to the edge of the cloud. The IF lies about 1' to the SW of S140 IRS1 and coincides closely with the outermost CO contour shown in Figure 1. The [CII]158μm has been observed by Boreiko et al. (1990) at the position of S140-IRS and at a point 30" SW. They suggested that the [CII] emission from S140 IRS1 originates from an HII region existing around a few of the embedded sources, while the emission from 30" SW derives from the PDR, excited by the star HD211880. Thermal continuum measurements at 50μm and 100μm were made by Lester et al. (1986) over a scale of 2' in RA and in Dec, centred on S140-IRS1. They found that the dust temperature reached a minimum between the embedded sources and the IF, indicating that the external radiation dominates the dust heating in the S and W scan directions. High resolution mapping at submillimetre wavelengths has also shown three peaks in emission centred around the cloud core (Minchin et al. 1995a). Grating spectra are reported here of the S140 region using the LWS instrument on board ISO (Kessler et al., 1996), covering the range 45μm to 187μm at a resolving power of between 150 and 300. A description of the LWS is given by Clegg et al. (1996) and its performance and calibration by Swinyard et al. (1996).

Send offprint requests to: R. Emery

[1] Based on observations with ISO, an ESA project with instruments funded by ESA Member States (specially the PI countries: France, Germany, the Netherlands and the United Kingdom) and with the participation of ISAS and NASA.

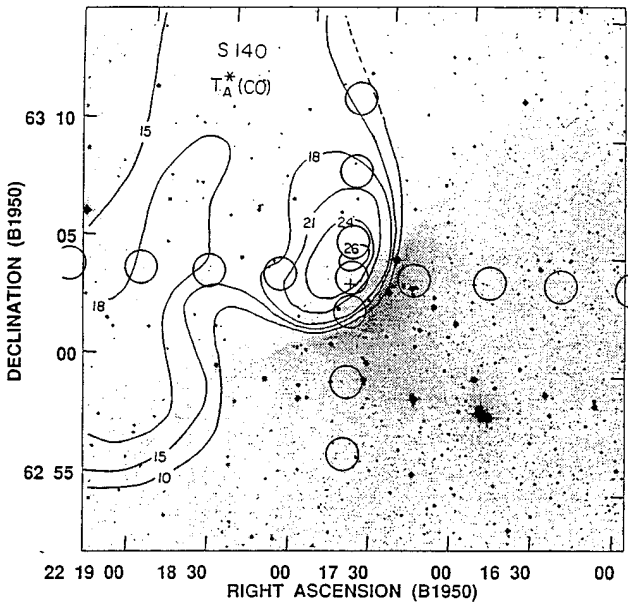

Fig. 1. LWS pointing positions used for the S140/L1204 region cuts, shown as 80" dia. circles, superposed on the CO map from Blair et al. (1978) and the Palomar Sky Survey

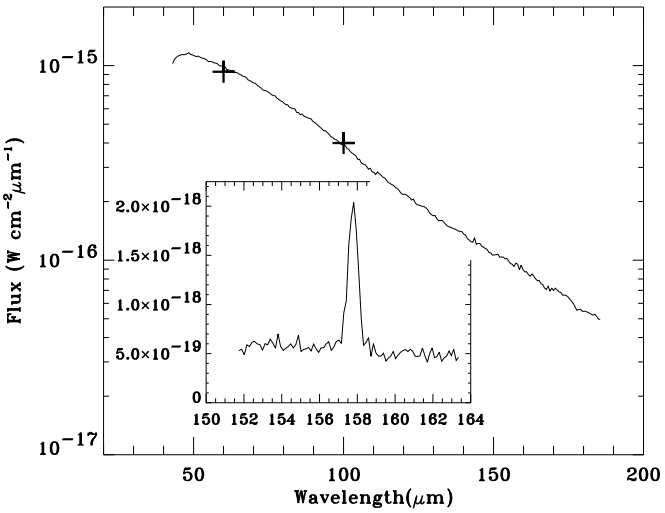

Fig. 2. Example of the full LWS spectrum at the central position (S140-IRS), covering 45 to 187μm. The lines are not easily seen at this position due to the very strong continuum emission. The inset shows the [CII] 158μm line on an expanded scale from a position 9' away from the centre where the continuum is a factor 1000 weaker. The crosses give the IRAS PSC values.

2. Observations.

The data described were taken during the routine observation phase of ISO, using the LWS01 observation mode with 4 samples per spectral element and fast scanning. Each spectrum was scanned 3 times with a nominal 0.25s integration time, giving an effective integration time of 0.45s per spectral sample. Figure 1 shows 15 of the 18 beam positions of the LWS (approximately 80" FWHM) superposed on the CO mapping of Blair et al. (1978), as represented by Zhou et al. (1994), also showing the same area of the Palomar Sky Survey. The pointings make up scans at constant RA and constant Dec, with 3' spacing, centred on the S140 IRS 1 position $\left(\propto 1950 = 22^h17^m41.1^s, \delta 1950 = 63^o3'42"\right)$ where the beam also contains the IRS 2 and IRS 3 sources. The beam positions not shown are an additional two positions further to the E and one position further to the W along the RA direction.

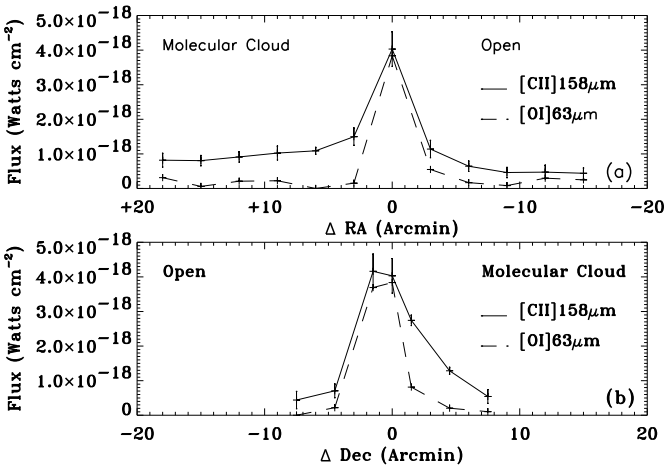

Fig. 3. Variation of [CII] 158μm and [OI]63μm line flux for cuts (a) at constant Dec. and (b) at constant RA, shown as ΔRA and ΔDec in arcminutes respectively from the central position on S140-IRSI

3. Results.

In Figure 2, the full LWS spectrum is shown for the central position. The continuum flux levels agree well with previous observations, as compiled by Zhou et al. (1994) and with the IRAS values, as does the total integrated luminosity for the $2-200\mu$m range of 1.8×10^4 solar luminosities, obtained using measurements with both of the ISO spectrometers. The [CII]158μm and the [OI]63μm emission lines are also seen at this position in the figure, but at low relative levels because of the very strong dust continuum emission. The inset shows the detail around the [CII] line from a spectrum obtained 9' away with low continuum emission and give an indication of the signal to noise ratio obtained on the line. Figure 3. (a) & (b) shows the fluxes of the [CII] and [OI] lines at each position along the constant Dec and constant RA cuts respectively. The peak flux for the [OI] line is observed towards the position centred on IRS1 and for the [CII] line towards the PDR/HII region interface. For the [CII] and [OI] lines the peak intensities are 3.5×10^{-4} and 3.3×10^{-4} erg s^{-1} cm^{-2} str^{-1} respectively. The peak [CII] flux is compared with the value of 3.6×10^{-4} erg s^{-1} cm^{-2} str^{-1} observed by Boreiko et al. (1990) for S140 IRS, with a beamwidth of about half that of the LWS, indicating that the majority of the flux is contained within this smaller field of view. The LWS observed continuum fluxes at the wavelengths of 50, 100, and 150μm, taken from the complete spectra, are presented in Figure 4. The peak flux,

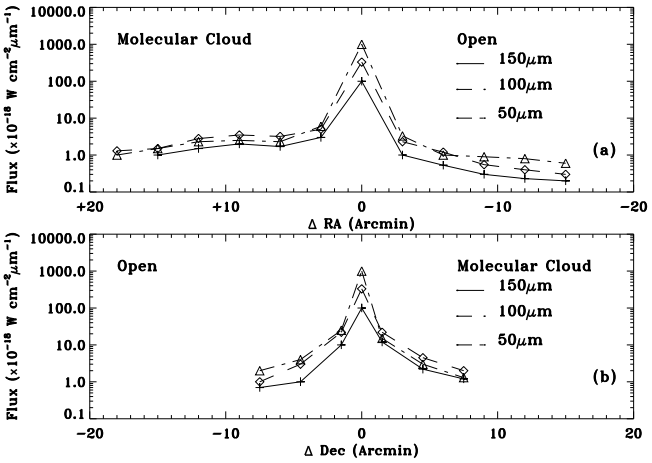

Fig. 4. Variation of thermal continuum flux (in units of $\times 10^{-18} W.cm^{-2}.\mu m^{-1}$) at wavelengths of 50, 100 and 150μm at the same beam position as shown in Figure 3

at the IRS source position, shows a level 10^3 times that of the surrounding material.

4. Discussion.

Fine-structure line emission from low ionisation states observed near HII regions arises primarily in photodissociation regions at the interface of ionized and molecular gas. Theoretical models often assume a one-dimensional homogenous structure for the PDR (Wolfire et al. 1990, Hollenbach et al. 1991) but cannot easily explain the large scale of the PDR line emission observed in many sources. A “clumpy" structure for the molecular cloud can alleviate this problem, as well as correct other discrepancies in the uniform models (Meixner et al. 1992, Meixner and Tielens 1993).

4.1. Fine Structure Emission

The [CII] and [OI] fine structure line fluxes shown in Figure 3 are roughly an order of magnitude lower than observed in other regions similar to S140 (Howe et al. 1991, Meixner et al. 1992). Thus the required UV fluxes to produce the emission lines are lowered, and embedded sources as well as ambient interstellar radiation may contribute significantly to any extended emission. If a density of 10^5 cm^{-3} is assumed for the central position, consistent with the CS observations of Zhou et al. (1994), the model results of Wolfire et al. (1990) require a UV field $100G_0$ or somewhat less (in units of 1.6×10^{-3} erg cm^{-2} s^{-1}) in order to give the [CII] line intensity observed here. At the measurement positions further into the molecular cloud, shown in Figure 1a, the [CII] flux is lower by a factor ~ 5 and for a wide range of lower densities, a uniform model predicts a correspondingly lower value of about $15G_0$.

If, away from the PDR, embedded sources contributed UV radiation, the flux distribution with distance would not be expected to be as smooth as observed here. Whether an ambient interstellar radiation field of $\sim 10G_0$ is present near the L1204 molecular cloud is also quite uncertain, and a clumpy molecular cloud is still the simplest way of explaining the very extended emission observed. If the UV radiation field from HD211880 impacted on a uniform region of density $> 3 \times 10^3$ cm^{-3}, the line emission would be limited to a region of less than 0.3 pc in extent, or less than 1’ at the distance of S140.

The line ratio [CII]158μm/[OI]63μm is an important diagnostic tool for PDR regions. ¿From the scans in Figure 3, this ratio is about unity at the central position, increasing to a value 3 - 10 for the measurement positions in the molecular cloud direction. Here, a uniform model with $\sim$ 10-100G_0, which is consistent with the [CII] flux in the cloud, then predicts a density for the PDR of $10^4 - 10^5$ cm^{-3} (Figure 1c of Wolfire et al.) As another check on the low values of radiation field, limits are obtained for the ratio of [OI]63μm/[OI]145μm of > 20 corresponding to values $< 10^3 G_0$ (Figure 1a of Wolfire et al.). On the other side, for positions further into the HII region, the ratio is in the range 2 - 6, which is consistent with higher radiation values for the lower densities. It is noted that in the N-S scan (Figure 3b), slightly more [CII] line emission is coming from the position at the IF than at the central position, while the [OI] line peaks at the central position. This may be due to the increased density seen in the CO map north of the IF, since the [OI] emission traces denser or more clumpy gas.

The fine structure line emission from the PDR regions in S140 thus seems to require a FUV non-ionizing radiation field (6 - 13.6 eV) of flux 0.2 erg cm^{-2}s^{-1} ($\sim 100G_0$) impacting on regions of density $10^4 - 10^5$ cm^{-3}. A B0V star of surface temperature 30,000K has a total non-ionizing luminosity of 4×10^4 solar luminosities, or a flux of 0.3 erg cm^{-2} s^{-1} at a distance of 2pc, the projected distance between HD211880 and the IF. The HII region surrounding HD211880, has a low density of the order of 10 cm^{-3}, and appears as a blister HII region slowly evaporating gas off the molecular cloud interface (Smirnov et al. 1995). Since hydrogen radio recombination lines were detected at projected distances $\sim$ 5pc from the star, Smirnov et al. (1995) suggested that the blister was behind or inside the molecular cloud. However, if the actual distance from the star to the PDR increases beyond 3 pc, the radiation field is inadequate in providing the observed CII emission at the central position for any density (cf. Figure 5 of Wolfire et al. 1990). Instead it may be that the star is off to the side, but close to the front edge (or back edge), and that its low density HII region provides the radio recombination lines from gas in front of (or back of) the molecular cloud.

For the ionising radiation, models of blister HII regions (Aannestad & Emery 1985) were used to calculate the ionization structure for a B0V star in an exponential density gradient of scale height 3 pc and a density of 13 cm^{-3} at the ionizing star. This used a recent model stellar atmosphere (Kurucz 1992) and also calculated the associated [CII] and [OI] line emissions from the blister, using a dust/hydrogen mass ratio of 0.009, typical of the interstellar value. The blister model is assumed to be seen edge-on, and the calculation gives $108G_0$ at the IF, which is at a distance of 2.2 pc from the star. The dust absorbs about

20% of the ionizing radiation from the star. The model gives line-of-sight [CII] emission values along the open RA scan of $(4-2)\times10^{-5}$ erg cm^{-2} s^{-1} sr^{-1} in good agreement with our observed values. The HII region therefore can account for the level of the extended [CII] emission shown in the open direction of Figure 3. HI clouds and hot intercloud gas along the line of sight would be expected to contribute only of the the order of $\sim 10^{-6}$ erg cm^{-2} s^{-1} sr^{-1} (Crawford et al. 1985). The observed [OI] emission in the open direction, however, is not accounted for by excitation with electrons in the IF, so may result from a weak shock front or from the warmer, denser gas surrounding the partially open blister.

4.2. Continuum Emission

The thermal emission from the heated dust, shown in Figure 4 for the wavelengths of 50, 100 and 150μm, also peak at the position of the embedded infrared sources, but are seen to peak much more sharply than the line emission (note the log scale). The ratio of the CII line flux to the total IR flux (Figure 2) is 5×10^{-5}, a value much lower than the value of $\sim 10^{-2}$ expected for low-density PDRs (Hollenbach et al 1991). At this position the embedded sources therefore dominate the IR emission but do not contribute to the CII line emission, which is instead driven by the external UV field. At the off-center positions, the IR emission comes from the re-emission by dust of the radiation from HD211880 in the molecular cloud, the PDR, and the HII region. However, in order to match the observed fluxes in the open direction, the blister calculation requires the HII region to be surrounded by a neutral gas envelope whose dust is contributing much of the FIR flux. The HII blister itself provides from 20 - 50% of the observed fluxes. Such an envelope may also provide some of the observed CII emission, but further modelling is required to determine its relative contribution.

The ratios of the fluxes gives the effective temperature of the dust, traced out from the relatively warmer dust in the HII region, through the PDR/HII region interface and the embedded sources, and into the relatively cold dust in the molecular cloud. The colour temperature based on the 50μm/100μm flux ratio at the central position is 40 - 50 K, depending on the emissivity law varying as λ^{-1} or as λ^{-2}. In the 'open' direction this temperature is between 35 and 45K, while in the molecular cloud direction it is about 30 - 35K. The latter values are in fair agreement with the 60μm/100μm colour temperature 'plateau' of about 27K, when stochastic heating of the dust is included (Hollenbach et al. 1991).

References

Aannestad P., Emery R., 1985, A&A 145, 347.
Blair G., et al., 1978, ApJ 219, 896.
Boreiko R. T., Betz A. L., Zmuidzinas J., 1990, ApJ 353, 181.
Clegg P. E., et al., 1996. this volume.
Crawford M.K., et al., 1985, ApJ 291, 755.
Crampton D., Fisher W.A., 1974, Pub. Dom. Astrophys. Obs. Victoria, 14, 283.
Hollenbach D. J., et al., 1991, ApJ, 377, 192.
Howe J. E., et al., 1991, ApJ, 373, 158.
Kessler M., et al. 1996, this volume.
Kurucz R. L., 1992, in The Stellar Populations of Galaxies, ed. B. Barbuy & A. Renzini (Dordrecht:Kluwer), p.225.
Lester D. F., et al., 1986, ApJ, 309, 80.
Meixner M., et al., 1992, ApJ 390, 499.
Meixner M., Tielens A., 1993, ApJ 405, 216.
Minchin N.R., et al., 1994, A&A 291, 250.
Minchin N.R., et al., 1995a, A&A 298, 894.
Minchin N.R., et al., 1995b, A&A 301, 894.
Plume R., Jaffe D.T.,Keene J., 1994, ApJ 425, L49.
Smirnov G. T., et al., 1995, A&A 300, 923.
Swinyard B. M., et al., 1996. this volume
Wolfire M.G., Tielens A., Hollenbach D., 1990, ApJ 358, 116.
Zhou S., et al., 1994, ApJ 428, 219.